Electronic Supplementary Material (ESI) for Journal of Materials Chemistry A
This journal is © The Royal Society of Chemistry

Electronic Supplementary Information

Fabrication of High-Stable Metal-Organic Frameworks and Corresponding Hydrophobic Foam through a Reticular Chemistry Strategy for Simultaneous Organic Micropollutant and Insoluble Oil Removal from Wastewater

Shuang Gai, Ruiqing Fan*, Jian Zhang*, Xuesong Zhou, Kai Xing, Ke Zhu, Wenwen Jia, Wenbo Sui, Ping Wang, and Yulin Yang*

MIIT Key Laboratory of Critical Materials Technology for New Energy Conversion and Storage, School of Chemistry and Chemical Engineering, Harbin Institute of Technology, Harbin 150001, P. R. of China

Corresponding Author: * Ruiqing Fan, Jian Zhang, and Yulin Yang

E-mail: fanruiqing@hit.edu.cn, zhaji@hit.edu.cn and ylyang@hit.edu.cn

Characterization

X-ray diffraction (XRD) patterns were recorded by using the Cu Kα radiation with a Shimadzu XRD-6000 X-ray diffractometer at 2θ recorded from 5–50°; Elemental analyses were obtained on a Perkin–Elmer 2400 automatic analyzer. And the Scan electron microscope (SEM) images were observed by Rili SU 8000HSD Series Hitachi New Generation Cold Field Emission SEM, where specific elemental species were analyzed by the X-ray energy dispersive spectrometer (EDS). The Fourier transform infrared spectroscopy (FT-IR) spectra data were collected by using a Nicolet impact 410 FT–IR spectrometer (4000-400 cm^{-1}). The zeta potential datas were measured through using a Zetasizer Nano-ZS90 (Malvern Instruments Ltd, U.K.). In addition, ultraviolet-visible absorption (UV-vis) spectra were collected on a Perkin-Elmer Lambda 20 spectrometer in the range of 200-800 nm at room temperature at 298K. X-ray photoelectron spectroscopy (XPS) analyses were performed on a PHI 5700 ESCA system using AlKa X-ray at 14 kV and 6 mA. Nitrogen sorption isotherms at 77K were measured on a Autosorb iQ Station 1 system. Before measurement, samples were pre-treated at 423 K for 10 h under nitrogen blowing. The specific surface area and the pore size distribution were calculated from the DFT data.

Single-crystal X-ray crystal structure determination

The single-crystal X-ray diffraction data of the crystals were collected on a Rigaku R-AXIS RAPID IP or a Siemens SMART 1000 CCD diffractometer equipped with graphite-monochromated Mo-Ka radiation (λ = 0.71073 Å). The crystal

structures were solved by direct methods and refined on F^2 by the full-matrix least squares by using the SHELXTL-2014 crystallographic software. Anisotropic thermal parameters were refined to all of the non-hydrogen atoms. The hydrogen atoms were fixed at calculated positions on carbon atoms and nitrogen atoms in ligands and refined by using a riding mode included water molecules.

Synthesis of $\{[Cd_3(bca)_3(H_2O)_2]\cdot H_2O\}_n$ (sql-M)

The synthesis of **sql-M** was used by a similar method which reported previously.[S1] A solution of $Cd(NO_3)_2\cdot 4H_2O$ (61.70 mg, 0.20 mmol), 1,3-H_2bca (1,3-benzenedicarboxylic acid) (16.60 mg, 0.10 mmol) in DMF (1.0 mL), CH_3OH (3.0 mL)and H_2O (2.0 mL) were added in a Teflon-lined stainless steel (20.0 mL) at 85 °C for 3 days. The colorless block crystals of **sql-M** were obtained after cooling to the room temperature and collected by filtrating, then washed by deionized water and dried in air.

Synthesis of $[Cd_{1.5}(btca)(H_2O)_3]_n$ (kia-M)

A solution of $Cd(NO_3)_2\cdot 4H_2O$ (61.70 mg, 0.20 mmol), H_3btca (1,3,5-benzenetricarboxylic acid) (21.01 mg, 0.10 mmol) in DMF (1.0 mL), CH_3CH_2OH (3.0 mL)and H_2O (2.0 mL), were added in a Teflon-lined stainless steel (20.0 mL) at 85 °C for 4 days. The colorless block crystals of **kia-M** were obtained after cooling to the room temperature and collected by filtrating, then washed by deionized water and dried in air. The crystal **kia-M** has been previously reported simply, but the description of **kia-M** was for comparing roundly.[S2]

Sample activation

All the prepared MOF samples were soaked in fresh N,N-Dimethylformamide

(DMF) for 12 h to remove the impurities and then guest exchanged for 12 h. This procedure repeated three times, subsequently, the samples were dried under a dynamic vacuum at 100 °C for 10 h for other experiments.

Batch aqueous-phase adsorption experiments

All CIP adsorption experiments were carried out on an orbital shaker at 180 rpm at 298 K. The mass of 6 mg of the adsorbent was added into the conical flasks with 20 mL of target CIP with the initial concentration (C_0) from 10 mg·L^{-1} to 60 mg·L^{-1}. In order to study the effect of different pH values for CIP adsorption, the initial CIP aquous solution (pH = 3 - 12) was adjusted by adding 1 M NaOH or 1 M HCl. The adsorbtion experiments was shaked last for 24 h to ensure adsorption equilibration. Then the sorbent was removed by filter (0.22 μm), and the residual mass of CIP were analyzed by UV-vis spectrophotometer at the wavelength of 268 nm.

Adsorption Kinetics

To study the adsorption kinetics of CIP on **Kgd-Zn**, 60 mg of **Kgd-Zn** was added to 200 mL of CIP aquous solutions (60 mg·L^{-1}) with constant magnetic stirring at 298K for a scheduled time (5-1440 min). Then, 4 mL of solutions were collected at predetermined time intervals and filtered to remove the adsorbents by a 0.22 μm filter. The UV-vis spectrums of solutions were analyzed by UV-vis spectrophotometer at the wavelength of 268 nm, respectively.

Absorption measurements of oil and organic solvents

The absorption measurement methods were carried out according to the reported process by Meng and co-workers.[S3] A weighted quantity of the **Kgd-Zn** and **Kgd-**

Zn@MF was immersed and kept static for 2 minutes in various oils and organic solvents to reach the adsorption equilibrium at room temperature. Afterwards, the extra solvent was removed by dropper from the sample vial, and the remaining weight of the mixtures was quickly weighed to avoid evaporation of the absorbed oils and organic solvents. The absorption capacity of the samples was calculated by the following equation: $(W_b-W_a)/W_a \times 100\%$. W_a and W_b are the weight of **Kgd-Zn** and **Kgd-Zn**@MF before and after oil or organic solvents absorption, respectively. It should be noted that the saturation adsorption could be observed by naked eyes, in addition, the experimental error was estimated to be less than 1 drop of added/removed liquid with a relative error of below 8%.

Simultaneous removal of ciprofloxacin and oil

The simulative multiple pollutants wastewater was prepared by mixing the 5 $mg \cdot L^{-1}$ of CIP (9.9 mL) and 1 vol % of soybean oil (0.1mL). The prepared mixed solution was sonicated for 30 min. Afterwards, **Kgd-Zn**@MF for water purification experiments were carried out at 298 K.

Table S1. Selected bond distance (Å) for **kgd-Zn**.

kgd-Zn					
Zn(1)-O(6)#1	2.089(2)	Zn(1)-O(7)#5	2.096(2)	O(5)-Zn(2)#6	1.927(2)
Zn(1)-O(6)#2	2.089(2)	Zn(2)-O(3)	1.922(2)	O(6)-Zn(1)#6	2.089(2)
Zn(1)-O(4)#3	2.091(2)	Zn(2)-O(5)#2	1.927(2)	O(7)-Zn(1)#7	2.096(2)
Zn(1)-O(4)	2.091(2)	Zn(2)-O(8)#5	1.967(2)	O(8)-Zn(2)#7	1.967(2)
Zn(1)-O(7)#4	2.096(2)	Zn(2)-O(9)	1.988(2)		

Table S2. Selected bond angles (°) for **kgd-Zn**.

kgd-Zn					
O(6)#1-Zn(1)-O(6)#2	180.00(14)	O(6)#2-Zn(1)-O(7)#4	86.02(10)	O(7)#4-Zn(1)-O(7)#5	180.0
O(6)#1-Zn(1)-O(4)#3	93.36(10)	O(4)#3-Zn(1)-O(7)#4	93.25(9)	O(3)-Zn(2)-O(5)#2	132.73(11)
O(6)#2-Zn(1)-O(4)#3	86.64(10)	O(4)-Zn(1)-O(7)#4	86.75(9)	O(3)-Zn(2)-O(8)#5	116.90(11)
O(6)#1-Zn(1)-O(4)	86.64(10)	O(6)#1-Zn(1)-O(7)#5	86.02(10)	O(5)#2-Zn(2)-O(8)#5	98.52(11)
O(6)#2-Zn(1)-O(4)	93.36(10)	O(6)#2-Zn(1)-O(7)#5	93.98(10)	O(3)-Zn(2)-O(9)	101.02(10)
O(4)#3-Zn(1)-O(4)	180.00(13)	O(4)#3-Zn(1)-O(7)#5	86.75(9)	O(5)#2-Zn(2)-O(9)	101.05(11)
O(6)#1-Zn(1)-O(7)#4	93.98(10)	O(4)-Zn(1)-O(7)#5	93.25(9)	O(8)#5-Zn(2)-O(9)	101.88(11)

Table S3. The parameters of pseudo-first-order kinetic and pseudo-second-order kinetic of CIP adsorption.

	pseudo-first-order			pseudo-second-order		
MOFs	q_e ($mg \cdot g^{-1}$)	K_1 (min^{-1})	R^2	q_e ($mg \cdot g^{-1}$)	K_2 ($g \cdot mg^{-1} \cdot min^{-1}$)	R^2
kgd-Zn	14.3	0.0033	0.406	165.8	0.00124	0.999

Table S4. The parameters of Langmuir model and Freundlich model of CIP adsorption.

	Langmuir model			Freundlich model		
MOFs	q_{max} ($mg \cdot g^{-1}$)	K_L ($L \cdot mg^{-1}$)	R^2	n	K_F ($mg^{-1/n} \cdot L^{1/n} \cdot g^{-1}$)	R^2
kgd-Zn	239.2	0.2220	0.997	1.617	44.1459	0.971

Table S5. Comparison of adsorption capacities with other reported adsorbents.

Adsorbent	Temperature (°C)	q_e(mg·g^{-1})	References
MIL-101(Cr)/Fe_3O_4	25	63.3	S4
$[Cu(Glu)_2(H_2O_2)]H_2O$	25	61.35	S5
DDMGO	35	230	S6
Fe-MCM-41	35	93.8	S7
Multi-walled CNTs	25	192.4	S8
Kgd-Zn	25	239.2	This work

Table S6. The property of ciprofloxacin.

Ciprofloxacin Structure	Molecular Formula	pK_a
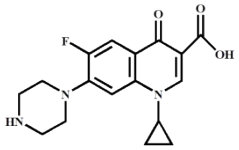	$C_{17}H_{18}FN_3O_3$	pK_{a1} = 5.9 pK_{a2} = 8.9

Table S7. The residual amount of Zn^{2+} ions of **kgd-Zn** in the filtered solutions

Condition	the amount of Zn^{2+} (ppb)
	kgd-Zn
HCl solutions (pH=2)	1.816
NaOH solution (pH=12)	2.047
water treatment for 7 days	1.012

Table S8. Comparison of adsorption capacities with other reported adsorbents

Adsorbent	Absorption substances	Oil adsorption capacity (wt%)	References
Porous BN nanosheets	Ethanol, toluene, pump oil, used engine oil, ethylene glycol	2000-3300	S9
TZC5	Chloroform, n-hexane, 1,2-DCB, THF, acelone, ethanol, methanol, kerosene, gasoline, pump oil	1000-2300	S10
MGS aerogel	cyclohexane, olive oil, soybean oil, vacuum pump oil, liquid paraffin, chloroform	6800-13000	S11
modified sponge with TiO_2 and octadecanoic acid	hexane, isooctane, dodecane, tetrachloromethane, toluene, dichloromethane	2700-6000	S12
Hollow SiO_2/MnO_2 cube coated PU foam	Diesel, pump oil, soybean oil, DMF, acetone, THF, toluene	800-3200	S13
MS@TiO_2@PPy	n-hexane, cyclohexane, methylbenzene, tetrachloromethane	4480-11070	S14
FGO@MOG	CCl_4, crude oil, decane, hepatane, hexane, octadecane, octane, petrolether, pentane, toluene, veg oil	200-500	S15
OctA/rGA aerogel	Pump oil, DCM, Chloroform, Hexadecane, Ethylbenzene, Cyclohexane, p-Xylene, Hexane, Toluene, Benzene	4700-16122	S16
ZIF-8@rGO@Sponge	n-Heptane, ethyl acetate, dibromoethane, butanone, acetone, toluene, tetrachloromethane, chloroform, silicone oil, bump oil, bean oil	1400-3700	S17
LA-3D-RB-β-NiOOH@sponge	n-hexane, soybean oil, chloroform, methylbenzene, lubricating oil, dichloromethane	571-936	S18
Kgd-Zn@MF	Petroleum ether, cyclohexane, chloroform, soybean oil, n-hexane, dichloromethane, veg oil, pump oil	5077 - 13786	This work

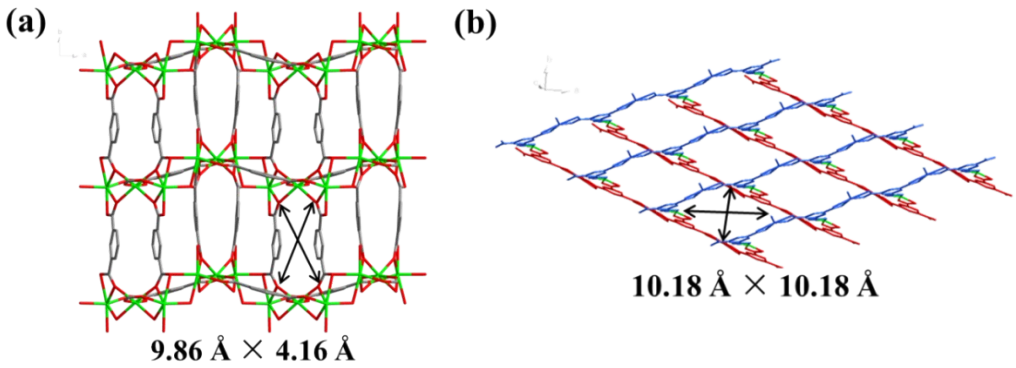

Fig. S1. (a) 2D layer of **sql-M** and a square pore structure with a size of 9.86 Å × 4.16 Å; **(b)** 2D layer of **kia-M** and a square pore structure with a size of 10.18 Å × 10.18 Å.

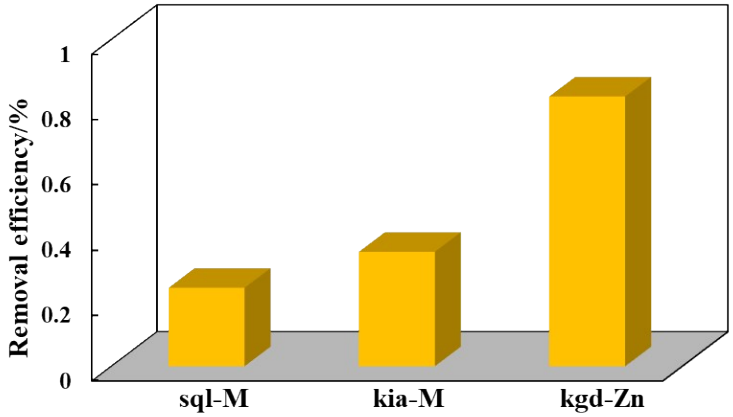

Fig. S2. Removal efficiencies toward CIP by **sql-M**, **kia-M** and **kgd-Zn**.

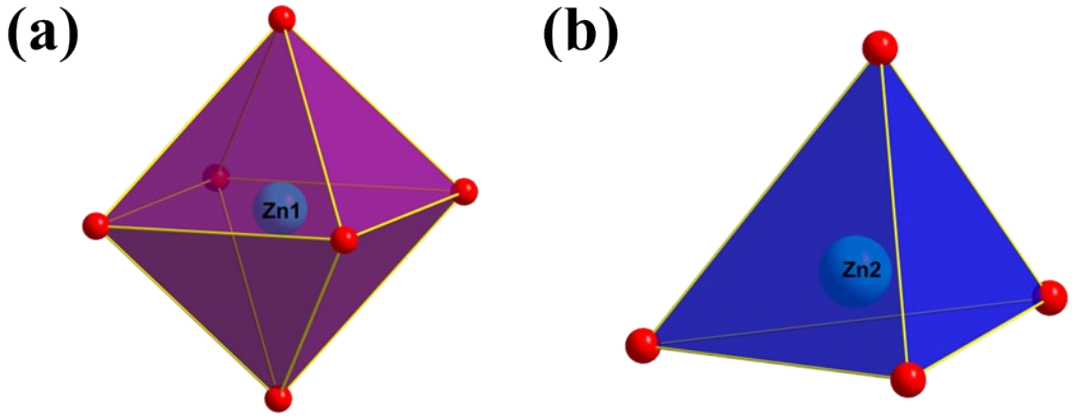

Fig. S3. Polyhedral representation of the coordination sphere of the Zn^{2+} center in **kgd-Zn** (water molecules and hydrogen atoms are omitted for clarity).

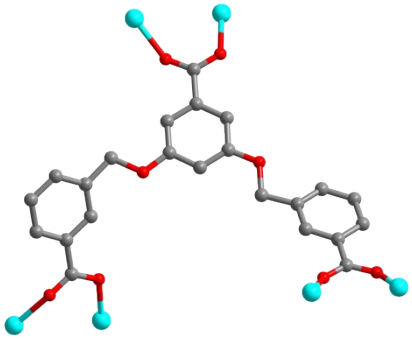

Fig. S4. The connection mode of the bcoba^{3-} ligand in **kgd-Zn**.

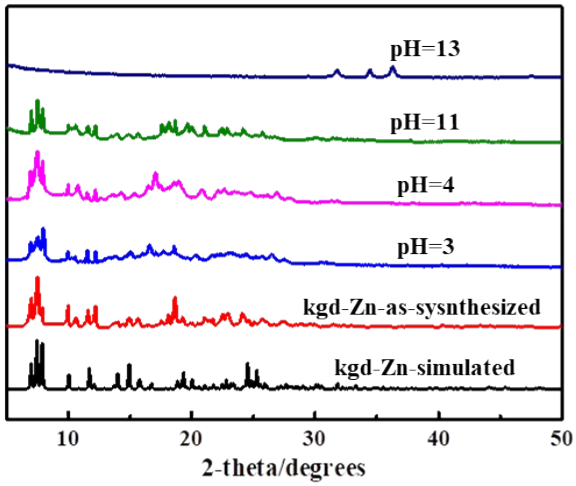

Fig. S5. The PXRD patterns of samples after soaked in acid or basic solutions, respectively.

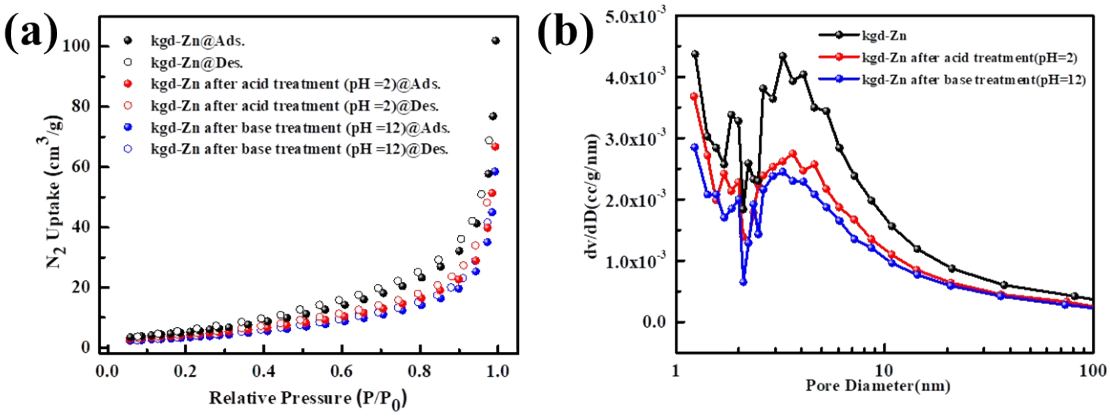

Fig. S6. (a) N_2 adsorption/desorption isotherms of **kgd-Zn** after treated in the NaOH solution (pH=12) and HCl solutions (pH=2), respectively, at 77 K; (b) DFT pore size distribution for the corresponding MOFs.

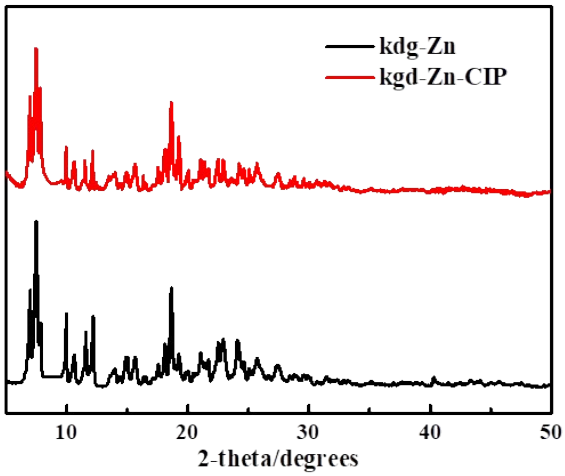

Fig. S7. The PXRD pattern of **kgd-Zn** before and after CIP adsorption.

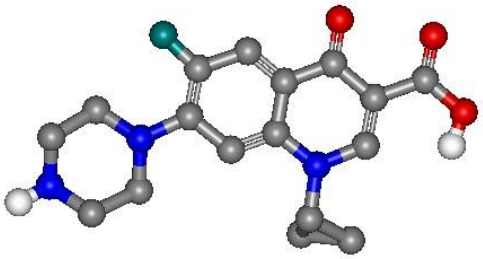

Fig. S8. Molecular structures of the CIP.

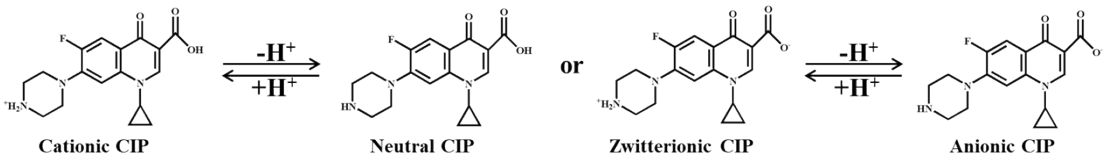

Fig. S9. The speciation of process reactive for CIP in aqueous solution as a function of the solution pH.

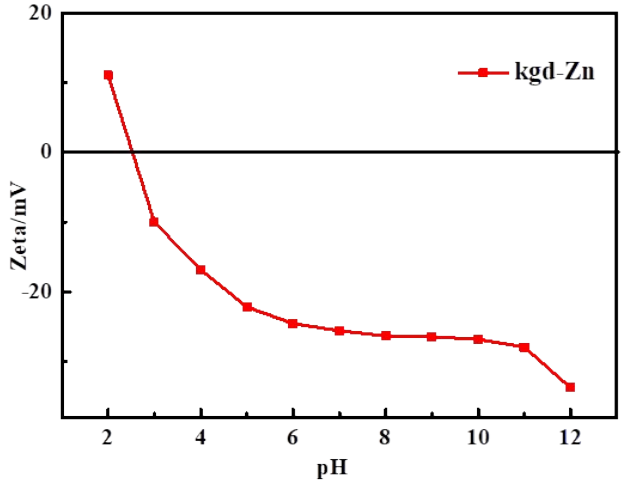

Fig. S10. The zeta potential of **kgd-Zn**.

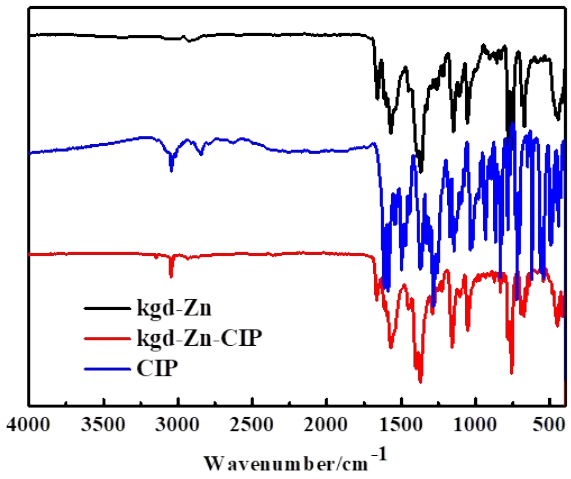

Fig. S11. FTIR spectra of CIP, **kgd-Zn** and **kgd-Zn** adsorbed CIP.

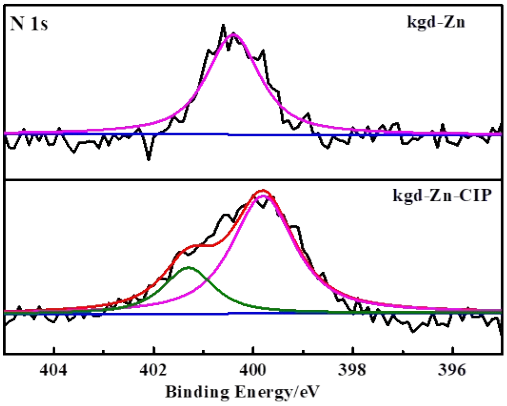

Fig. S12. N 1s spectra of **kgd-Zn** before (upper lines) and after (lower lines) adsorption.

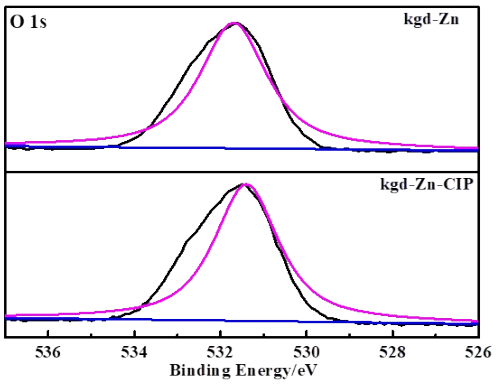

Fig. S13. O 1s spectra of **kgd-Zn** before (upper lines) and after (lower lines) adsorption.

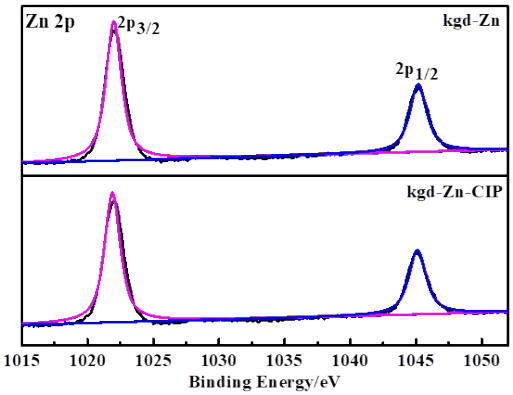

Fig. S14. Zn 2p spectra of **kgd-Zn** before (upper lines) and after (lower lines) adsorption.

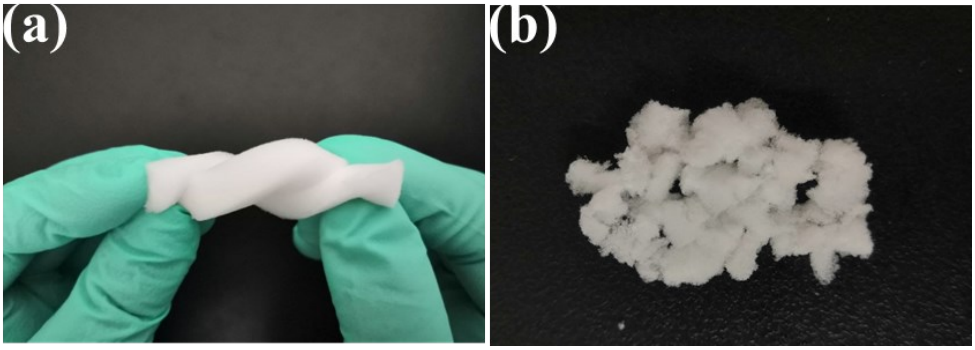

Fig. S15. Digital camera image of (a) compressed melamine foam and (b) teared melamine foam.

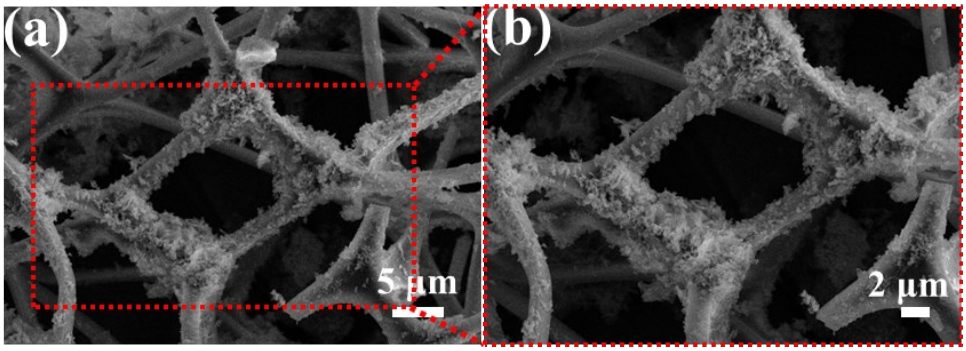

Fig. S16. SEM images of **kgd-Zn1**@MF.

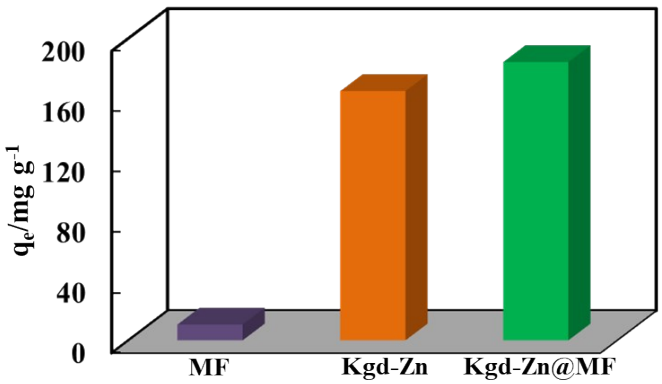

Fig. S17. Adsorption uptakes of CIP by MF, **kgd-Zn** and **kgd-Zn**@MF.

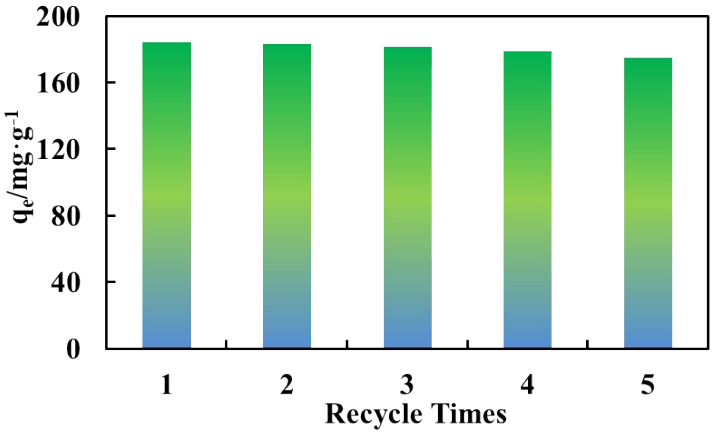

Fig. S18. Recycling adsorption of CIP by **kgd-Zn**@MF.

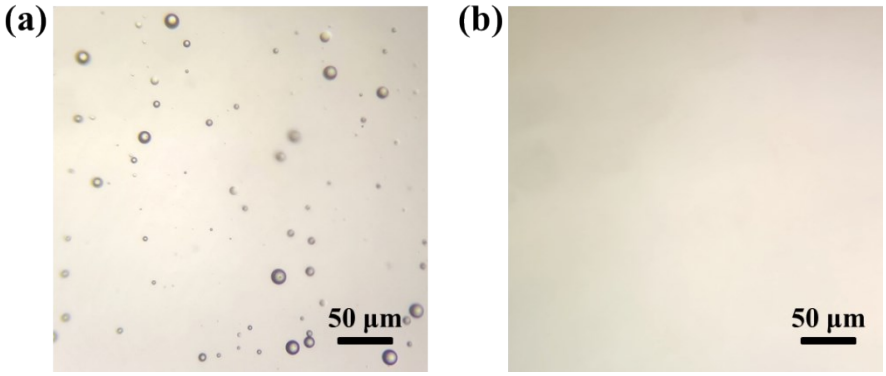

Fig. S19. The microscopy images of the soybean oil/water mixture (a) after and (b) before filtration.

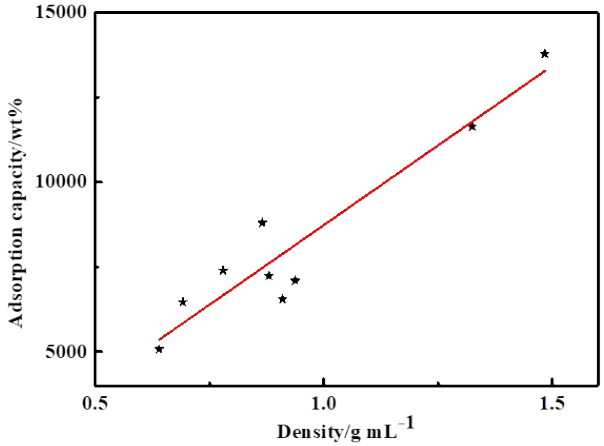

Fig. S20. Adsorption capacities of **kgd-Zn**@MF measured for a range of oils and organic solvents in terms of the solvent densities.

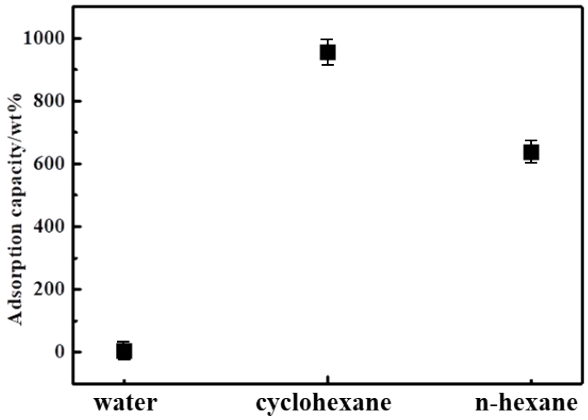

Fig. S21. Absorption capacities of **kgd-Zn** toward water, hexane and cyclohexane.

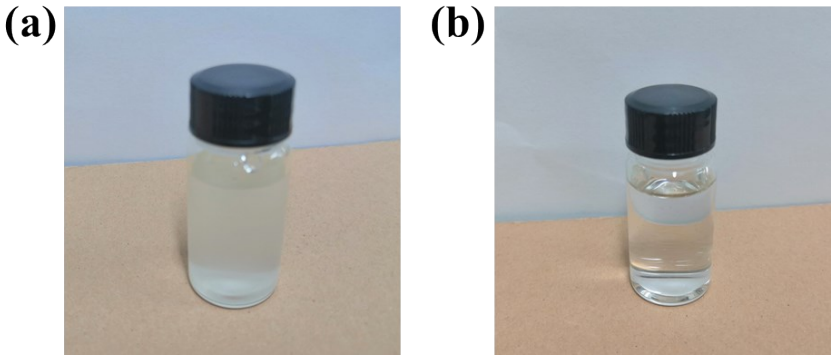

Fig. S22. Photographs of simulated wastewater containing 1 vol% soybean oil, 5 mg·L^{-1} CIP (a) before and (b) after filtration.

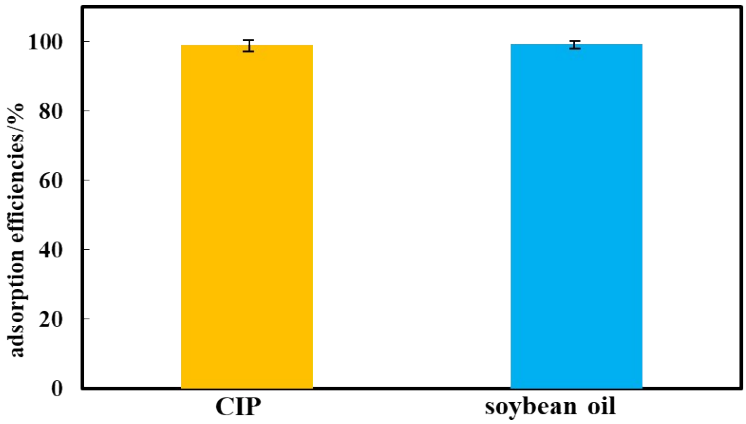

Fig. S23. Simultaneous removal performance toward CIP and soybean oil by **kgd-Zn**@MF.

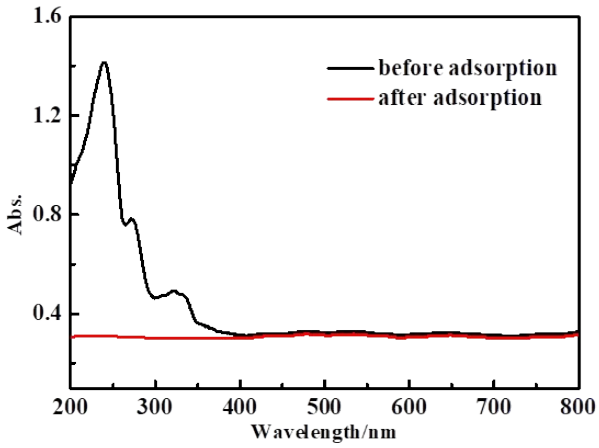

Fig. S24. UV-Vis spectra of the simulated wastewater containing 5 mg·L^{-1} CIP and 1 vol% soybean oil before and after filtration.

References

[S1] F. Luo, Y. -X. Che, J. -M. Zheng, *J. Coord. Chem.*, 2010, **61**, 2097-2104.

[S2] M. Xue, G. S. Zhu, L. F. Wang, Q. R. Fang, J. Y. Sun, F. X. Sun, X. D. Guo, X. J. Zhao, G. Tian, S. L. Qiu, *Chemical Journal of Chinese Universities-Chinese*, 2005, **26**, 2211-2213.

[S3] J. H. Gu, H. W. Fan, C. X. Li, Jürgen Caro, H. Meng, *Angew. Chem., Int. Ed.*, 2019, **58**, 5297-5301.

[S4] S. S. Bayazit, S. T. Danahoğlu, M. A. Salam, Ö. K. Kuyumcu, Environ. Sci. Pollut. Res., 2017, **32**, 25452-25461.

[S5] M. D. Olawale, A. C. Tella, J. A. Obaleye, J. S. Olatunji, *New J. Chem.*, 2020, **44**, 3961-3970.

[S6] M. F. Li, Y. G. Liu, S. B. Liu, G. M. Zeng, X. J. Hu, X. F. Tan, L. H. Jiang, N. Liu, J. Wen, X. H. Liu, *J. Colloid Interface Sci.*, 2018, **521**, 150-159.

[S7] Y. Wu, Y. Tang, L. Li, P. Liu, X. Li, W. Chen, Y. Xue, *Front. Chem.*, 2018, **6**, 17-28.

[S8] F. Yu, S. Sun, S. Han, J. Zheng, J. Ma, *Chem. Eng. J.*, 2016, **285**, 588-595.

[S9] W. W. Lei, D. Portehault, D. Liu, S. Qin, Y. Chen, *Nat. Commun.*, 2013, **4**, 1777-1784.

[S10] J. H. Kim, J. Y. Oh, J. M. Lee, Y. C. Jeong, S. H. So, Y. S. Cho, S. Nam, C. R. Park, S. J. Yang, *Carbon*, 2018, **126**, 190-196.

[S11] Q. Wang, Y. Qin, C. Xue, H. Yu, Y. Li, *Chem. Eng. J*,. 2020, **402**, 126240.

[S12] L. Li, L. Liu, J. Lei, J. He, N. Li, F. Pan, *J. Mater. Chem. A*, 2016, **4**, 12334-12340.

[S13] D. Yuan, T. Zhang, Q. Guo, F. Qiu, D. Yang, Z. Ou, *Chem. Eng. J.*, 2017, **327**, 539–547

[S14] Y. S. Lee, B. K. Kaang, N. Han, H.-J. Lee, W. S. Choi, *J. Mater. Chem. A*, 2018, **6**, 16371-16381.

[S15] K. Jayaramulu, F. Geyer, M. Petr, R. Zboril, D. Vollmer, R. A. Fischer, *Adv. Mater.*, 2017, **29**, 1605307-1605313

[S16] S. H. Eom, D. W. Kang, M. J. Kang, J. H. Choe, H. Kim, D. W. Kim, C. S. Hong, *Chem. Sci.*, 2019, **10**, 2663-2669.

[S17] J. H. Gu, H. W. Fan, C. X. Li, J. Caro, H. Meng, Chen, *Angew. Chem. Int. Ed.*, 2019, **58**, 5297-5301.

[S18] M. Li, X. Xu, L. Zhang, *J. Ind. Eng. Chem.*, 2020, **84**, 340-348.